

X-ray Tests of General Relativity with Black Holes

Cosimo Bambi 

Center for Field Theory and Particle Physics, Department of Physics, Fudan University, Shanghai 200438, China; bambi@fudan.edu.cn

Abstract: General relativity is one of the pillars of modern physics. For decades, the theory has been mainly tested in the weak-field regime with experiments in the solar system and radio observations of binary pulsars. Until 2015, the strong-field regime was almost completely unexplored. Thanks to new observational facilities, the situation has dramatically changed in the last few years. Today, we have gravitational wave data of the coalesce of stellar-mass compact objects from the LIGO-Virgo-KAGRA collaboration, images at mm wavelengths of the supermassive black holes in M87* and Sgr A* from the Event Horizon Telescope collaboration, and X-ray data of accreting compact objects from a number of X-ray missions. Gravitational wave tests and black hole imaging tests are certainly more popular and are discussed in other articles of this Special Issue. The aim of the present manuscript is to provide a pedagogical review on X-ray tests of general relativity with black holes and to compare these kinds of tests with those possible with gravitational wave data and black hole imaging.

Keywords: black holes; general relativity; astrophysical tests of gravity; X-ray astronomy; Kerr metric

1. Introduction

The theory of general relativity is one of the pillars of modern physics. The theory was proposed by Einstein at the end of 1915 [1] and in more than 100 years it has passed a large number of observational tests without requiring any modification from its original version [2]. The first test of general relativity can be dated back to 1919, when Eddington and collaborators measured the effect of light bending by the Sun during a solar eclipse [3]. After that observation, Einstein and his theory soon became very popular, but the precision and the accuracy of that measurement were actually quite poor and that experiment was not really able to distinguish general relativity from alternative scenarios. Systematic tests of general relativity started only in the 1960s with experiments in the solar system and in the 1970s with accurate radio observations of binary pulsars [2]. Solar system experiments and radio pulsar observations can mainly test the *weak-field regime*, where the astrophysical system can be described as a Newtonian system plus some small corrections. With those tests, we want to measure such small corrections and check whether they are consistent with the predictions of general relativity. In the past 20 years, there have been significant efforts to test general relativity on *large scales* (galactic scales or above) in response to the problems of dark matter and dark energy [4–6]. Until some years ago, the *strong-field regime* was almost completely unexplored. However, since 2015 the situation has dramatically changed. Today, we can probe the strong-field regime with gravitational wave data from the LIGO-Virgo-KAGRA collaboration (see, e.g., Refs. [7–9]), images of the supermassive black holes in M87* and Sgr A* from the Event Horizon Telescope collaboration (see, e.g., Refs. [10–12]), and X-ray data from a number of X-ray missions (see, e.g., Refs. [13–15]).

Black holes are ideal laboratories to test the strong-field regime as they are the sources of the strongest gravitational fields that can be found today in the universe [16,17]. In 4-dimensional general relativity, black holes are relatively simple objects and are completely described by a small number of parameters. This is the celebrated result of the *no-hair theorem*, which is actually a family of theorems with different versions and a number of extensions [18]. According to the no-hair theorem, astrophysical black holes should be



Citation: Bambi, C. X-ray Tests of General Relativity with Black Holes. *Symmetry* **2023**, *15*, 1277. <https://doi.org/10.3390/sym15061277>

Academic Editor: Rahul Kumar Walia

Received: 20 May 2023

Revised: 10 June 2023

Accepted: 16 June 2023

Published: 18 June 2023



Copyright: © 2023 by the author. Licensee MDPI, Basel, Switzerland. This article is an open access article distributed under the terms and conditions of the Creative Commons Attribution (CC BY) license (<https://creativecommons.org/licenses/by/4.0/>).

characterized only by their mass, spin angular momentum, and electric charge. Since the electric charge is normally negligible for macroscopic astronomical objects, the mass and the spin should be the only two parameters relevant for astrophysical black holes and the spacetime metric should be described by the Kerr solution [19]. Deviations from the Kerr metric due to the presence of an accretion disk, nearby stars, or a non-vanishing equilibrium electric charge can be estimated, but normally they turn out to be completely negligible; see, e.g., Refs. [17,20,21]. For example, a non-vanishing equilibrium electric charge is a natural consequence of the difference between the values of the masses of electrons and protons as well as of their different photon scattering cross-sections. However, the value of the equilibrium electric charge turns out to be completely negligible for the spacetime geometry around a black hole; for more details, see, for instance, Section 6.5.2 in Ref. [17]. On the other hand, the conclusion of the no-hair theorem can be easily invalidated in extensions of general relativity (see, e.g., [22]) if macroscopic quantum gravity effects show up in the vicinity of these compact objects (see, e.g., [23,24]), or in the presence of exotic matter fields (see, e.g., [25,26]).

There are already some recent reviews on tests of general relativity with black hole X-ray data; see, for instance, Ref. [27], where the interested reader can find more details and a long discussion on the systematic uncertainties of this kind of measurements. The aim of the present manuscript is to provide a shorter and more easily accessible review on the topic. In particular, Section 3 shows the physics involved in the calculations of synthetic black hole spectra and how we can modify these calculations to test new physics. While X-ray tests are not as popular as tests with gravitational wave data and black hole imaging, they can provide very competitive constraints, at least comparable and complementary to those from gravitational waves and certainly stronger than those from black hole imaging.

2. Disk-Corona Model

To test general relativity with black hole X-ray data, we need to study very special systems. To have a rough idea of how unique these systems are, we can consider the stellar-mass black holes in our Galaxy. From stellar population and evolution studies, we expect that there are 10^8 – 10^9 stellar-mass black holes formed from the collapse of heavy stars in our Galaxy [28]. On the other hand, we know less than 100 stellar-mass black holes that (more often sporadically, for short times, from weeks to months) have an accretion disk sufficiently bright to be studied with our X-ray observatories. Some of these black holes have been studied well and we have hundreds of observations from different X-ray missions, while for other objects we have only a few observations. Among thousands of X-ray observations of stellar-mass black holes in our Galaxy, we have to select the sources and the observations suitable for testing general relativity, and in the end we find that there are only a few spectra from the most recent X-ray missions that can do the job!

The prototype of astrophysical system for our tests is shown in Figure 1 (for more details, see [29] and references therein). The black hole can be either a stellar-mass black hole in an X-ray binary system or a supermassive black hole in an active galactic nucleus. This black hole is surrounded by a *cold*, geometrically thin, and optically thick accretion disk. Such a disk forms when the angular momentum of the accreting material is high and the mass accretion rate is between a few percent and about 30% of the Eddington limit of the central object. In these conditions, every point on the surface of the accretion disk emits a blackbody-like spectrum and the whole disk has a multi-temperature blackbody-like spectrum, because the temperature of the accreting material increases as the radial distance from the black hole decreases. The thermal spectrum of the disk is normally peaked in the soft X-ray band (0.1–10 keV) for stellar-mass black holes in X-ray binary systems and in the UV band (1–100 eV) for supermassive black holes in active galactic nuclei. The “corona” is some *hot* (~ 100 keV) gas around the black hole and the inner part of the accretion disk: the corona may be the base of the jet, some atmosphere above the accretion disk, hot material in the plunging region between the inner edge of the accretion disk and the black hole, etc. Since the disk is cold and the corona is hot, thermal photons from the accretion disk can

inverse Compton scatter off free electrons in the corona. These Comptonized photons have a spectrum that can be normally approximated well by a power law with an exponential high-energy cutoff. Such a power law component is often the dominant component in the X-ray spectra of accreting black holes. Some Comptonized photons can illuminate the accretion disk: Compton scattering and absorption followed by fluorescent emission generate the so-called reflection spectrum.

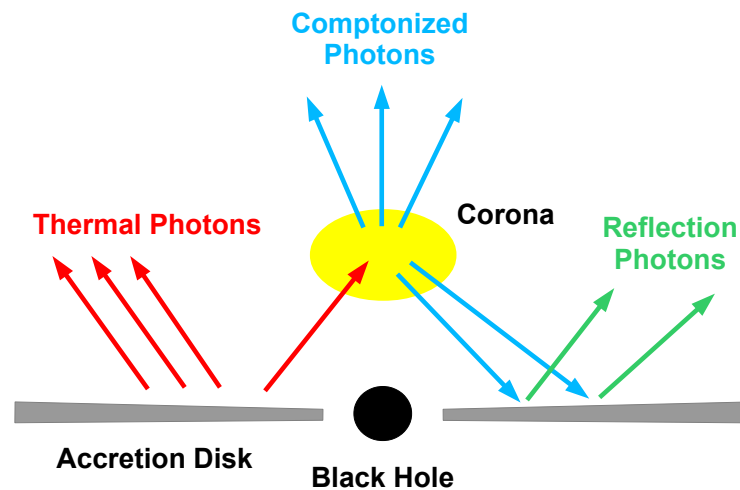


Figure 1. Disk-corona model. The black hole is surrounded by a cold, geometrically thin, and optically thick accretion disk. The corona is some hot gas near the black hole and the inner part of the accretion disk. Thermal photons from the disk inverse Compton scatter off free electrons in the corona. Some Comptonized photons illuminate the accretion disk and produce the reflection spectrum. Figure from Ref. [30] under the terms of the Creative Commons Attribution 4.0 International License.

The reflection spectrum in the rest-frame of the material of the disk is characterized by narrow fluorescent emission lines in the soft X-ray band and a Compton hump with a peak at 20–30 keV [31,32]. The most prominent emission line is normally the iron $K\alpha$ line, which is at 6.4 keV in the case of neutral or weakly ionized iron atoms and shifts up to 6.97 keV in the case of hydrogen-like iron ions. The reflection spectrum of the disk observed far from the source is blurred by relativistic effects (gravitational redshift and Doppler boosting) [17,33].

3. Synthetic Black Hole Spectra

In order to understand how we can use black hole X-ray data to test fundamental physics, it can be useful to briefly review how we calculate synthetic spectra of accreting black holes. We can consider the set-up illustrated in Figure 2, where we have the distant observer, the accretion disk, and the corona. These calculations are extensively discussed in the literature; see, for example, Ref. [17] and references therein. In this section, I only outline the basic steps, without showing any formulae.

The first step is to calculate the *redshift image* of the accretion disk. We fire photons from the image plane of the distant observer backward in time to the accretion disk. When a photon hits the disk, we calculate its redshift $g = E_o/E_e$, where E_o is the photon energy measured at the detection point in the rest-frame of the distant observer and E_e is the photon energy at the emission point in the rest-frame of the gas in the disk. To achieve this, we have to:

1. solve the equations of motion of the photons (the geodesic equations if we are considering a metric theory of gravity [2]) in order to connect every point of the observer's image of the disk to its emission point on the disk and calculate the photon 4-momentum at the emission point;
2. calculate the motion of the material in the disk (which should depend on the accretion disk model and on the equations of motion of the particles of the disk) in order to

determine the gas 4-velocity at the emission point (which, together with the photon 4-momentum at the emission point determined at point 1 above, is used to calculate the photon energy at the emission point in the rest-frame of the gas in the disk, E_e).

The details of these calculations can be found, for example, in Refs. [17,34]. At the end of the calculations, one has the redshift image of the accretion disk. If the photon's equations of motion are independent of the photon energy (as is the case in general relativity and any other metric theory of gravity), every point of the observer's image of the accretion disk has a well defined redshift (if not, then every point of the observer's image of the accretion disk has a redshift that depends on the photon energy).

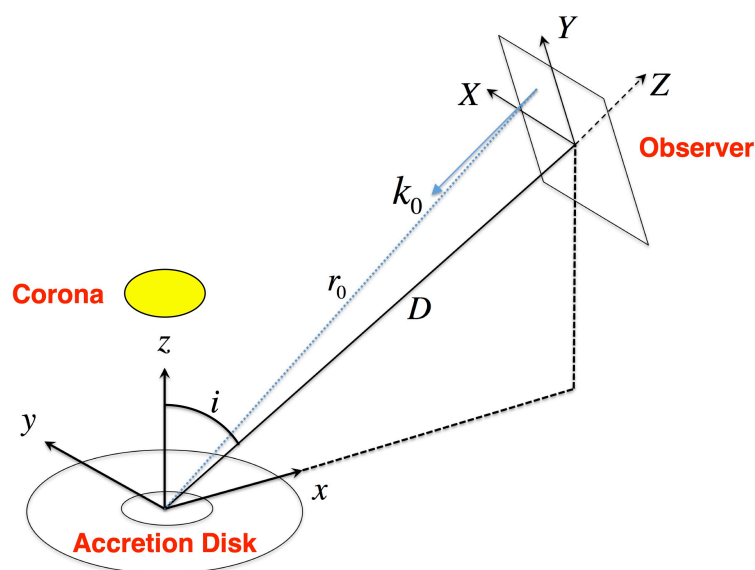


Figure 2. Set-up to calculate the spectrum of the accretion disk observed far from the source. See the text for more details. Figure adapted from Ref. [34].

The second step is to calculate the emissivity profile of the disk. In the case of the thermal component, current models employ Novikov–Thorne disks [35,36] and the emissivity profile is determined by the spacetime metric and the mass accretion rate. In the case of the reflection component, the emissivity profile is determined by the geometry and the emissivity of the corona. If we know these properties of the corona, we can fire photons from the corona to the accretion disk and calculate the emissivity profile of the reflection spectrum. These calculations are similar to those at step 1 and require solving the equations of motion of the photons from the corona to the disk and to determine the motion of the material in the disk. Unfortunately, the properties of the corona are not yet well understood. Current reflection models often do not assume a specific coronal geometry and employ some phenomenological emissivity profiles (such as a power law, broken power law, or twice broken power law) that are thought to be able to approximate well the emissivity profile generated by any possible coronal geometry.

The third and last step is to calculate the spectrum at the emission point in the rest-frame of the material of the disk. In the case of the thermal component, the spectrum is simply a blackbody spectrum with possible corrections due to the disk atmosphere (mainly photon-electron scattering). In the Novikov–Thorne model, the temperature at every radius of the disk is determined by an equation that follows from the conservation of mass, energy, and angular momentum and depends on the spacetime metric and the mass accretion rate. In the case of the reflection spectrum, we have to solve radiative transfer equations and the calculations involve atomic physics and some assumptions about the structure of the accretion disk. In general relativity, and in any other metric theory of gravity, the atomic physics in the strong gravitational field around a black hole is the same as the atomic physics in our laboratories on Earth. This is because locally the laws of non-gravitational

physics are those of special relativity in all metric theories of gravity. However, this is not the case in some theories of gravity, where the values of some fundamental constants (e.g., the fine structure constant α , the electron mass m_e , etc.) can be different in strong and weak gravitational fields; see, e.g., Refs. [27,37,38]. This may have an impact on the atomic energy levels, photon-electron scattering, etc., and, in turn, on the reflection spectrum of the disk [39].

In conclusion, the calculations of the thermal and reflection components require some assumptions about the astrophysical system (at least a model for the accretion disk, but the calculation of the reflection spectrum would also require a model for the corona) and some assumptions about fundamental physics (motion of photons and of particles around the compact object and atomic physics in strong gravitational fields). If the astrophysical part is well understood, we can think of testing the assumptions related to fundamental physics. Note that the Comptonized spectrum from the corona cannot be used to test fundamental physics, at least for the moment. The main reason is that we do not know the actual properties of the corona (geometry, temperature, location). The analysis of the thermal and reflection spectra can instead be used to test fundamental physics because the properties of geometrically thin and optically thick accretion disks are thought to be well understood.

In the last few years, my group at Fudan University has developed two models for testing fundamental physics with black hole X-ray data: `relxill_nk` [34,40] and `nkbb` [41]. `relxill_nk` is an extension of the `relxill` package developed by Thomas Dauser and Javier Garcia [42–44] and can calculate reflection spectra of accretion disks in stationary, axisymmetric, and asymptotically flat spacetimes. `nkbb` is instead a model for thermal spectra of accretion disks in stationary, axisymmetric, and asymptotically flat spacetimes. Both models are public and available on GitHub at <https://github.com/ABHModels> (accessed on 10 June 2023). They can be used with standard X-ray data analysis packages such as XSPEC.

4. Observational Constraints

There are two main strategies to test fundamental physics (in our case with black hole X-ray data, but actually this is true in general). These two strategies are normally referred to as the *top-down* (or theory-specific) approach and the *bottom-up* (or theory-agnostic) approach.

The top-down strategy is the most natural and logical one. In this case, we want to test some specific theory of gravity against general relativity. We can thus construct an astrophysical model for general relativity and another astrophysical model for the other theory of gravity, analyze some astrophysical data with the two models, and eventually we use some statistical tool to check if one of the two models can explain the data better than the other model (or in the most common case in which we want to test an extension of general relativity that includes general relativity in some special limit, we can measure and constrain the values of the parameters of the theory). The main drawback of this method is that it requires knowing well the predictions of the theory to test, but this is not so easy. For example, we may want to test a theory of gravity in which the spacetime metric of astrophysical black holes is expected to be different from the Kerr solution of general relativity. In such a case, we need to know the rotating black hole solution of that theory, but in most cases we only know the non-rotating black hole solutions of theories beyond general relativity simply because it is easier to find a static and spherically symmetric solution rather than a stationary and axisymmetric one. Note that this is true even in general relativity. The Schwarzschild solution describing static and spherically symmetric black holes in general relativity was found by Schwarzschild a few months after Einstein had presented his theory, while the Kerr solution was found by Kerr only in 1963 [19].

In the bottom-up (or agnostic) approach, we parametrize possible deviations from the predictions of general relativity. For example, if we want to test the prediction that the spacetime metric around astrophysical black holes is described by the Kerr solution, we can analyze astrophysical data with a model employing a black hole metric in which some

deformation parameters quantify possible deviations from the Kerr geometry and we can recover the Kerr solution for specific values of these deformation parameters. From the analysis of astrophysical data, we can infer the values of these deformation parameters and check whether they are consistent with the Kerr solution. If, on the other hand, we want to test the value of the fine structure constant in the strong gravitational field of black holes, we can analyze astrophysical data with a model employing synthetic reflection spectra calculated for different values of α . From the analysis of observations with this model, we can estimate the value of the fine structure constant near black holes. The main drawback of the bottom-up strategy is that normally we do not have a sufficiently general model to take into account any possible deviations from the predictions of general relativity. For example, we can use a certain deformed Kerr metric to test the Kerr hypothesis, but we do not have the most general black hole metric that can describe any possible deviation from the Kerr solution.

Up to now, most X-ray tests of general relativity with black holes have tested the Kerr hypothesis, namely, if the spacetime metric around astrophysical black holes is described by the Kerr solution. In the literature, we can find examples of theory-agnostic tests as well as of theory-specific tests. Tests beyond the Kerr hypothesis are somewhat more complicated and may be explored in coming years. For example, in Ref. [45] we tested the weak equivalence principle with the bottom-up approach considering the possibility that either the motion of X-ray photons or the motion of the particles in the disk can deviate from the geodesic motion in the Kerr metric, and we constrained possible violations of the weak equivalence principle with a *NuSTAR* observation of the stellar-mass black hole in EXO 1846–031. A very preliminary study to use the analysis of the reflection spectrum to measure the value of the fine structure constant in the strong gravitational field of black holes was reported in Ref. [39] but without deriving any constraint from observations.

4.1. Agnostic Tests of the Kerr Hypothesis

Since the 1960s, many experiments in the solar system have tested the Schwarzschild solution in the weak-field regime with the agnostic method. One can write the most general static and spherically symmetric line element as an expansion in M/r , where M is the mass of the central object and r is some radial coordinate. In isotropic coordinates, such a line element should read

$$ds^2 = -\left(1 - \frac{2M}{r} + \beta \frac{2M^2}{r^2} + \dots\right) dt^2 + \left(1 + \gamma \frac{2M}{r} + \dots\right) (dx^2 + dy^2 + dz^2) \quad (1)$$

in order to recover the correct Newtonian limit. In Equation (1), β and γ are unknown parameters to be determined by observations. If we write the Schwarzschild metric in isotropic coordinates, we find that $\beta = \gamma = 1$. We can analyze experiments in the solar system employing the metric in Equation (1) to measure β and γ . As of now, solar system experiments can confirm that the value of these two parameters is 1 with a precision at the level of 10^{-5} , which confirms the Schwarzschild solution in the weak-field regime within the precision of current experiments [2].

In a similar spirit, we can try to test the Kerr solution around astrophysical black holes. Unfortunately, we cannot use an expansion in M/r because we want to probe the strong gravity region where M/r is not a small parameter. At least for the moment, we do not have a general framework as in the case of solar system experiments. In the literature, there are a number of *parametric black hole spacetimes* specifically proposed to test the Kerr hypothesis with electromagnetic data; see, for instance, Refs. [46–52] for a non-complete list of options. Every proposal has its advantages and disadvantages. One of these parametric black hole spacetimes is the Johannsen metric [47], which has been extensively used for testing general relativity with X-ray data as well as with other techniques. In Boyer–Lindquist-like coordinates, the line element of the Johannsen metric is

$$\begin{aligned}
 ds^2 = & -\frac{\Sigma(\Delta - a^2 A_2^2 \sin^2 \theta)}{B^2} dt^2 + \frac{\Sigma}{\Delta A_5} dr^2 + \Sigma d\theta^2 \\
 & + \frac{[(r^2 + a^2)^2 A_1^2 - a^2 \Delta \sin^2 \theta] \Sigma \sin^2 \theta}{B^2} d\phi^2 \\
 & - \frac{2a[(r^2 + a^2) A_1 A_2 - \Delta] \Sigma \sin^2 \theta}{B^2} dt d\phi, \quad (2)
 \end{aligned}$$

where

$$\Sigma = r^2 + a^2 \cos^2 \theta, \quad (3)$$

$$\Delta = r^2 - 2Mr + a^2, \quad (4)$$

$$B = (r^2 + a^2) A_1 - a^2 A_2 \sin^2 \theta \quad (5)$$

and the functions f , A_1 , A_2 , and A_5 are defined as

$$f = \sum_{n=3}^{\infty} \epsilon_n \frac{M^n}{r^{n-2}}, \quad A_1 = 1 + \sum_{n=3}^{\infty} \alpha_{1n} \left(\frac{M}{r}\right)^n, \quad (6)$$

$$A_2 = 1 + \sum_{n=2}^{\infty} \alpha_{2n} \left(\frac{M}{r}\right)^n, \quad A_5 = 1 + \sum_{n=2}^{\infty} \alpha_{5n} \left(\frac{M}{r}\right)^n. \quad (7)$$

The Johannsen metric has four infinite sets of deformation parameters: $\{\epsilon_n\}$ ($n = 3, 4, \dots$), $\{\alpha_{1n}\}$ ($n = 3, 4, \dots$), $\{\alpha_{2n}\}$ ($n = 2, 3, \dots$), and $\{\alpha_{5n}\}$ ($n = 2, 3, \dots$). This form of the Johannsen metric has the correct Newtonian limit and cannot be distinguished from the Schwarzschild metric by solar system experiments (for this reason there are not ϵ_1 , ϵ_2 , α_{11} , α_{12} , α_{21} , and α_{51}). α_{13} is the leading order correction to Kerr spacetime as well as the parameter with the strongest impact on the spectra of thin disks, and for this reason most tests of the Kerr hypothesis have focused on the constraints on the value of this parameter.

Figure 3 shows some reflection spectra of thin disks in the Johannsen spacetime for different values of the deformation parameter α_{13} calculated with `relxill_nk`. Figure 4 shows some thermal spectra of thin disks in the Johannsen spacetime calculated with `nkbb`. In both cases, all the other parameters of the models are kept constant and different spectra are simply obtained by changing the value of the deformation parameter α_{13} (while all other deformation parameters of the Johannsen metric vanish). The red spectra with $\alpha_{13} = 0$ are those in the Kerr metric. As we can see from Figures 3 and 4, the value of the deformation parameter α_{13} has a clear impact on the shape of the reflection and thermal spectra. It is thus clear that we can use `relxill_nk` and `nkbb` to analyze X-ray spectra of accreting black holes and, modulo degeneracy with other parameters, we can measure α_{13} .

Figure 5 compares the current measurements of the Johannsen deformation parameter α_{13} obtained from the analysis of X-ray data with `relxill_nk` and `nkbb`, with the analysis of gravitational wave data, and from black hole imaging. We distinguish tests of the Kerr hypothesis with stellar-mass black holes from those with supermassive black holes, as they can potentially probe different regimes. In the case of the constraints from reflection features and gravitational wave data, only the most precise and accurate measurements on α_{13} are shown in Figure 5.

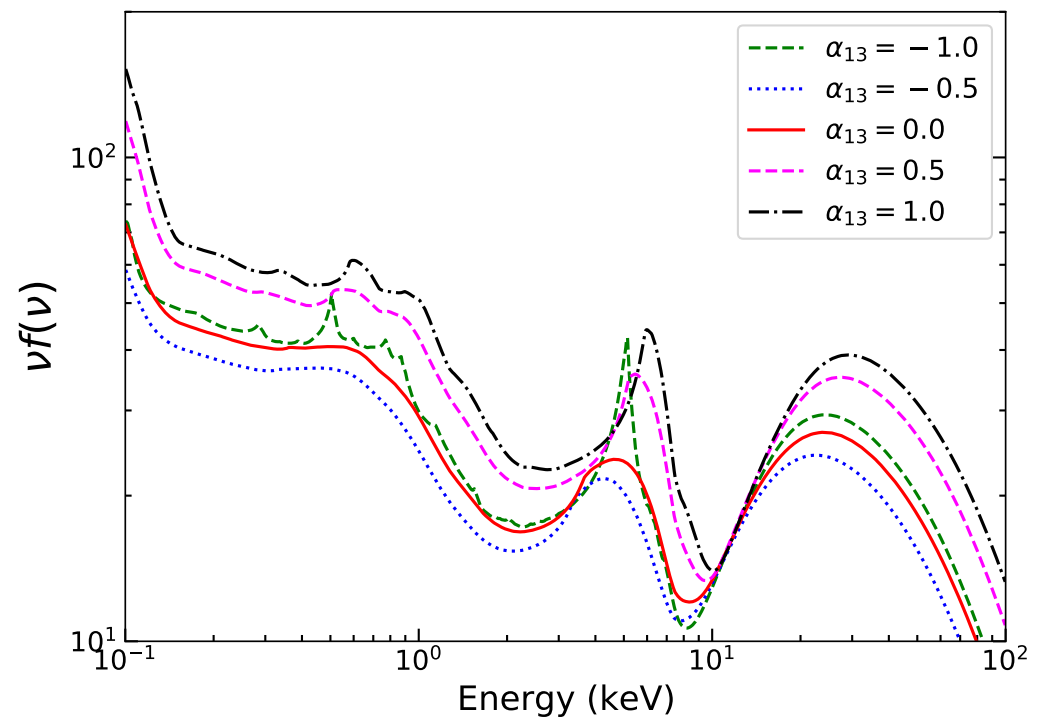


Figure 3. Synthetic reflection spectra of thin disks in the Johannsen spacetime for different values of the deformation parameter α_{13} . The values of the other model parameters are not changed. Figure from Ref. [30] under the terms of the Creative Commons Attribution 4.0 International License.

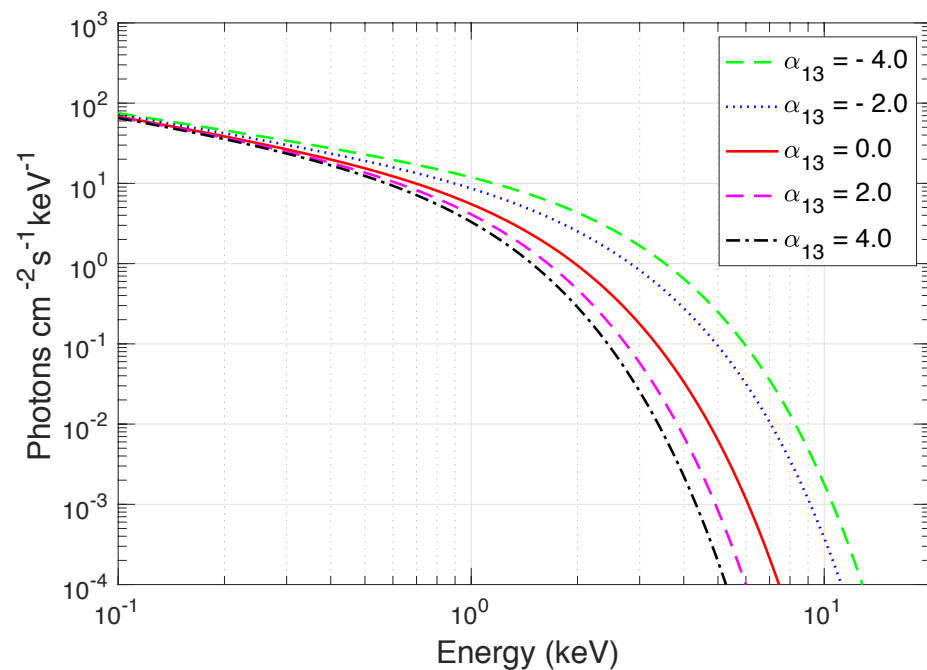


Figure 4. Synthetic thermal spectra of thin disks in the Johannsen spacetime for different values of the deformation parameter α_{13} . The values of the other model parameters are not changed. Figure from Ref. [41].

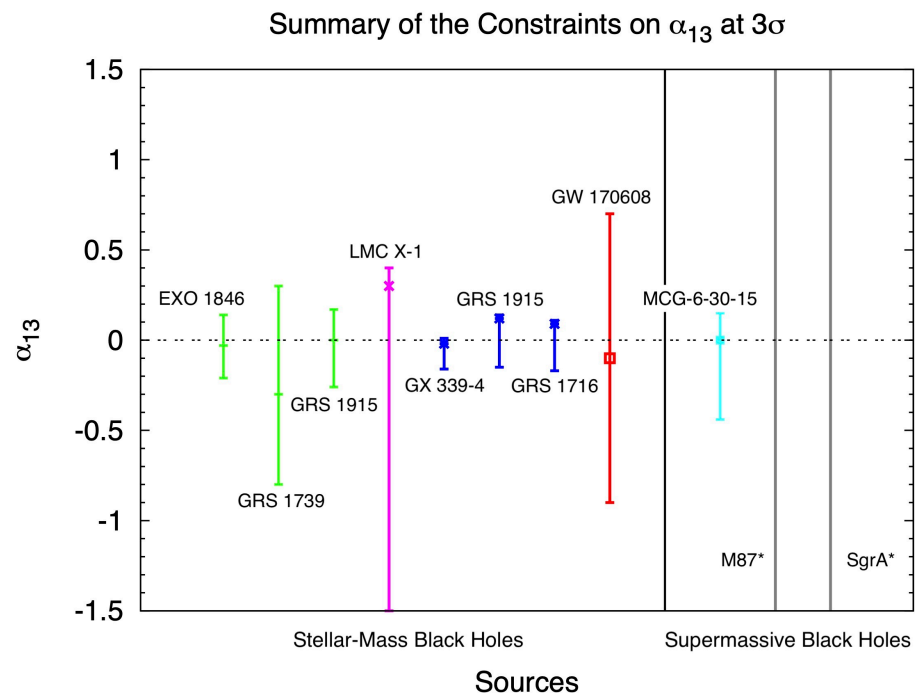


Figure 5. Summary of current measurements of the Johannsen deformation parameter α_{13} with different techniques. Every measurement shows the best-fit value, the $3\text{-}\sigma$ upper and lower uncertainties, and the name of the source. The constraints in green are the three most precise and accurate measurements of α_{13} for stellar-mass black holes from the analysis of the reflection features using `relxill_nk` (EXO 1846–031 [15], GRS 1739–278 [15], and GRS 1915+105 [53,54]). The constraint in magenta is the measurement of α_{13} for the stellar-mass black hole in LMC X-1 from the analysis of thermal spectra using `nkbb` [55]. The constraints in blue are obtained combining the analysis of the reflection features with `relxill_nk` and of the thermal spectrum with `nkbb` for the same source (GX 339–4 [56], GRS 1915+105 [57], and GRS 1716–249 [58]). The constraint in red is the most precise measurement of α_{13} for stellar-mass black holes with gravitational wave data [59]. The constraint in cyan is the most precise and accurate measurement of α_{13} for supermassive black holes from the analysis of reflection features using `relxill_nk` (MCG–6–30–15 [14]). Last, the two constraints in gray are from black hole imaging for the supermassive black holes M87* [11] and Sgr A* [60] (in both cases, the authors do not report the best-fit values but only the allowed α_{13} ranges, which are larger than the range $(-1.5, 1.5)$ shown in this figure). The horizontal dotted line at $\alpha_{13} = 0$ marks the Kerr solution of general relativity. Figure adapted from Ref. [61].

The most stringent constraints to date are from the simultaneous analysis of reflection features and thermal spectra of the stellar-mass black holes in GX 339–4, GRS 1915+105, and GRS 1716–249 (blue data in Figure 5). In general, the sole analysis of the thermal spectrum cannot constrain a deformation parameter well because the thermal spectrum has a very simple shape (see Figure 4): even if we know the mass and the distance of the source, we cannot constrain simultaneously the spin, the mass accretion rate, and the deformation parameter (see the magenta constraint in Figure 5 and the discussion in Ref. [55]). For supermassive black holes, the thermal spectrum is peaked in the UV band, where dust absorption prevents any accurate measurement and, therefore, we cannot use the analysis of the thermal spectrum and `nkbb` to test supermassive black holes. In general, we can obtain stronger constraints from stellar-mass black holes than from supermassive black holes (the sources are brighter and normally their spectra are not affected by absorption of material crossing our line of sight, even if their hotter disks are more difficult to model). However, MCG–6–30–15 is an exceptional case (cyan bar in Figure 5): the source is very bright, its spectrum has often a very strong and broadened iron line, and the constraint on α_{13} is obtained from the analysis of high-quality simultaneous observations, *NuSTAR*

and *XMM-Newton*, that combine a broad energy spectrum and a high energy resolution in the iron line region. In the end, the constraint on α_{13} from MCG–6–30–15 is comparable to the best constraints from stellar-mass black holes with only `relxill_nk` (green data). The red constraint from gravitational wave data of the coalescence of two stellar-mass black holes is obtained following the approach proposed in Ref. [62], where one assumes that the gravitational wave emission is the same as in general relativity and the constraint on α_{13} only comes from the motion of the bodies; within an agnostic approach, it could not be otherwise, because here we only know the spacetime metric—in this specific case, the Johannsen metric with the deformation parameter α_{13} —and we do not know the field equations of the theory. These parametric black hole spacetimes are obtained by deforming the Kerr solution following certain criteria; they are not the exact solutions of specific gravity theories. The best gravitational wave constraint on α_{13} is weaker than the best X-ray constraints, but for other deformations from the Kerr solution we may find opposite results [59,63,64]. This is understandable because X-ray and gravitational wave tests are sensitive to very different physics and different relativistic effects, so X-ray tests can constrain better some deformations from the Kerr geometry and gravitational wave tests can constrain better other deformations. Last, we have the constraints from M87* and Sgr A* (gray data in Figure 5) from black hole imaging. These constraints are definitely weaker than those from X-ray and gravitational wave tests. They may be able to reach the current sensitivity of X-ray and gravitational wave tests with the launch of a telescope to space; such a possibility is already discussed within the community and could improve the current angular resolution by an order of magnitude.

4.2. Theory-Specific Tests of the Kerr Hypothesis

`relxill_nk` has even been used to test specific theories of gravity in which electrically neutral black holes are not described by the Kerr solution. In the end, this technique is quite general. We just need to implement the correct black hole metric in `relxill_nk` and then analyze some reflection-dominated black hole spectra to measure the parameters of the theory.

In Einstein–Maxwell dilaton–axion gravity, black holes are expected to have a dilaton charge $r_2 \geq 0$ and the Kerr solution of general relativity is recovered when $r_2 = 0$. In Ref. [65], we analyzed a *NuSTAR* observation of the stellar-mass black hole in EXO 1846–031 and we inferred the following constraint on r_2

$$r_2 < 0.011 \quad (90\% \text{ CL}). \quad (8)$$

Conformal gravity is a family of theories beyond general relativity that have been proposed to solve the problem of spacetime singularities [66–68]. The singularity-free black holes in conformal gravity are characterized by a new parameter, $L > 0$. For $L = 0$, we recover the singular Kerr solution of general relativity. From the analysis of black hole X-ray data with `relxill_nk` we can infer the following constraint on L/M (where M is the black hole mass) [69,70]

$$L/M < 0.09 \quad (90\% \text{ CL}). \quad (9)$$

If we quantize general relativity, we obtain an effective quantum field theory valid only at energies much lower than the Planck scale. Asymptotically safe quantum gravity is a promising candidate scenario to provide a UV extension for such an effective field theory of general relativity. In Ref. [71], the authors proposed a rotating black hole metric in asymptotically safe quantum gravity. Such a solution is characterized by a new parameter, $\tilde{\gamma} > 0$, which is inversely proportional to the asymptotically safe fixed-point value of the theory. The Kerr metric is recovered when $\tilde{\gamma} = 0$. In Ref. [72], we implemented such a rotating black hole metric in asymptotically safe quantum gravity in `relxill_nk` and we analyzed a *Suzaku* observation of the stellar-mass black hole in GRS 1915+105. From our analysis, we measured $\tilde{\gamma}$

$$\tilde{\gamma} < 0.047 \quad (90\% \text{ CL}). \quad (10)$$

The constraint on $\tilde{\gamma}$ from X-rays is much stronger than that obtained from black hole imaging in Ref. [71].

Even if we assume that general relativity is the correct theory of gravity, there is not yet a proof that the final product of the complete gravitational collapse of an uncharged body is a Kerr black hole. On the other hand, today we know exact solutions of the Einstein equations in which the complete collapse of a body does not produce a Kerr black hole and instead leads to a spacetime with naked singularities [73]. In Ref. [74], we explored the possibility that the spacetime around gravitationally collapsed objects is described by the δ -Kerr metric [75,76], which is an exact solution of the Einstein equations that can be obtained from a non-linear superposition of the δ -metric and the Kerr metric. The δ -Kerr metric has an extra parameter, q , which measures deviations from the Kerr solution. The Kerr metric is recovered for $q = 0$, while the object is more oblate (prolate) than a Kerr black hole if $q > 0$ ($q < 0$). Implementing the δ -Kerr metric in `relxill_nk` and analyzing the *NuSTAR* spectrum of the stellar-mass black hole in EXO 1846–031, in Ref. [74] we inferred the following constraint on q

$$-0.1 < q < 0.7 \quad (90\% \text{ CL}). \quad (11)$$

The examples reported in this sub-section are to show that `relxill_nk` is a tool that can normally test any theory of gravity in which we know the rotating black hole solution and it is different from the Kerr metric. We also note that the constraints inferred from the analysis of reflection spectra with `relxill_nk` are more stringent than the constraints inferred with other electromagnetic techniques. On the other hand, constraints from gravitational wave data are difficult to infer because they require precise calculations of gravitational waveforms in those theories, which are normally not well studied yet.

5. Accuracy of X-ray Tests of General Relativity

Are the X-ray tests of the Kerr hypothesis presented in the previous section robust? In Figure 5, we see that the X-ray measurements of the Johannsen deformation parameter α_{13} are certainly more precise than those with current gravitational wave data and black hole imaging, but are they also accurate?

The answer to this question is that we believe that these tests of the Kerr hypothesis with black hole X-ray data are robust, but we must be very careful to select the right sources and the right observations. The point is that we do not need to test as many sources as possible to obtain a large number of (accurate and inaccurate) measurements. We can instead focus on a small number of spectra that are thought to be well understood and can provide very precise measurements. Let us note that the situation is very different from most astrophysical studies, where, for example, we want to measure the spin parameter of as many sources as possible to study the spin distribution of a whole black hole population. Another example is the case in which we want to study a certain kind of accretion state of black holes, even if such a state is not ideal for precise measurements of the system. The situation is also very different from the tests with gravitational wave data and black hole imaging. In the case of gravitational wave data, all systems are quite similar and share the same systematic uncertainties in the measurement of their parameters (in the end, they are just two black holes in vacuum!); this is also evident from the fact that the constraints from different sources on possible deviations from the Kerr solution are all quite similar [59,62], while in the case of X-ray tests we can have sources that provide very strong constraints and sources that cannot provide constraints at all. In the case of black hole imaging, we have only M87* and Sgr A*, as the angular size of any other supermassive black hole in our sky is too small and, therefore, we have to understand those sources and their observations well even if they are not ideal for tests of fundamental physics.

Generally speaking, our tests with X-ray data require selecting sources in which (a) the signature of relativistic effects is strong in the spectrum, and (b) the accretion

process is well understood and constrained. Point (a) is necessary to break the degeneracy between possible new physics and the astrophysical model, as well as to have precise measurements/constraints of new physics. Point (b) is required to limit the systematic uncertainties of the astrophysical model. To be more specific, the sources and observations suitable for testing fundamental physics with the analysis of the reflection features should meet the following requirements:

1. The inner edge of the accretion disk should be as close as possible to the compact object. A necessary but not sufficient condition is that the spin parameter of the compact object is high (say, $a_* > 0.9$ if it is a Kerr black hole).
2. The corona should be compact and close to the compact object.
3. The accretion disk should be geometrically thin and optically thick, with the inner edge at or near the innermost stable circular orbit (ISCO). A necessary, but not sufficient, condition is that the Eddington-scaled accretion luminosity is between a few percent and about 30%.
4. The spectrum must have a prominent iron line.
5. The source must be bright (and the data should not be affected by pile-up).
6. The geometry of the accretion disk and of the corona should not change during the observation.
7. The X-ray data should cover both the iron line region and the Compton hump, and possibly have a good energy resolution in the iron line region.

Points 1 and 2 are necessary to have most of the reflection component generated very close to the black hole, so that the relativistic effects in the X-ray spectrum are stronger and thus they are more easy to measure with good precision; see also Refs. [27,42,77]. Since `relxill_nk` assumes that the accretion disk is thin and the motion of the gas is Keplerian, we must select the sources with such a disk, which is point 3 above. Simulations of reflection spectra from GRMHD-generated thin disks show that we can recover the correct input parameters well from the X-ray spectrum [78]. On the contrary, if we analyze sources with a too high mass accretion rate, the disk is thick, and we can easily obtain very precise, but inaccurate, measurements of the spacetime metric [79,80]. Since the shape of the iron $K\alpha$ line is the most informative part of the reflection spectrum for our tests, it is important to analyze data with prominent and very broadened iron lines, which is point 4 above. Note, for example, that in a fully ionized disk the iron line disappears in the X-ray spectrum of the source. If we select the right sources and the right observations, the uncertainty in the final measurement is dominated by the statistic uncertainty in the photon count, which decreases if the source is bright (point 5). If the geometry of the accretion flow in the strong gravity region or the geometry of the corona change during the observation, this should be taken into account in the data analysis process and it is definitively a complication. If the properties of the disk and the corona do not change, point 6, this simplifies the analysis. Last, it is certainly useful both to have a good energy resolution in the iron line region (because the shape of the iron line is the most informative part of the spectrum) and to analyze a broad spectrum, including the Compton hump (because this helps to constrain other parameters of the model, such as the ionization of the disk, and, in turn, even to obtain a better measurement of the spacetime metric around the black hole), which is point 7. For this reason, the constraints reported in Section 4 are mainly obtained from *NuSTAR* data (which permit fitting of the energy band 3–80 keV) or, as in the case of MCG–6–30–15, simultaneous observations of *NuSTAR* and *XMM-Newton* (which provide a good energy resolution in the iron line region).

6. Concluding Remarks

This article has summarized the state of the art of tests of general relativity with black hole X-ray data. In the past few years, we have developed the reflection model `relxill_nk` and the thermal model `nkbb` to test fundamental physics from the analysis of X-ray spectra of accreting black holes. So far, we have mainly worked on tests of the Kerr hypothesis; that is, to test if the spacetime metric around astrophysical black holes is

described by the Kerr solution as expected in the framework of standard physics (general relativity, no exotic matter fields, no naked singularities, etc.). In the future, these tests can be extended to study possible deviations from geodesic motion induced by new fields, violation of Lorentz invariance, new interactions between the gravity and the matter sectors, etc. While X-ray tests of general relativity are not as popular as tests with gravitational wave data or black hole imaging, they can provide very competitive constraints, usually somewhat stronger than those possible with current gravitational wave observations and certainly much stronger than those with current images of the supermassive black holes M87* and Sgr A*.

If we select carefully the sources and the observations, X-ray tests of the Kerr hypothesis can be robust, and in such a case the constraints on possible deviations from the Kerr solution are limited by the quality of the data. To improve significantly current X-ray constraints we have to wait for the next generation of X-ray missions, starting from *eXTP* [81] (currently scheduled to be launched in 2028). For example, an observation with *eXTP* can roughly improve the constraint on a deformation parameter by an order of magnitude with respect to a similar observation with *NuSTAR* of the same source [74]. However, in order to fully exploit the high-quality data from the next generation of X-ray missions, it will be necessary to develop more sophisticated theoretical models than those available today or, otherwise, we risk having very precise, but not very accurate, measurements of the space-time metric. Future models should include the effect of the returning radiation (i.e., the radiation emitted by the disk and returning to the disk because of the strong light bending near black holes), more accurate calculations of the reflection spectrum in the rest-frame of the material in the disk, more sophisticated descriptions of the emissivity profiles by implementing specific coronal geometries, and more sophisticated accretion disk models than the Novikov–Thorne one (probably employing GRMHD-generated accretion disks).

Gravitational wave tests promise to improve quickly in the near future and we can expect that eventually they will be able to put the most stringent constraints on the Kerr hypothesis (see, for instance, Ref. [82]). However, X-ray tests can still be interesting because they are complementary to the gravitational wave tests. X-ray tests can indeed probe better the interactions between the gravity and the matter sectors. For example, non-minimal coupling between the gravity and the matter sectors could induce deviations from geodesic motions of photons or some particle species, variation in fundamental constants in the strong gravity region around black holes, etc. These phenomena are more difficult or impossible to detect with gravitational wave data. On the other hand, gravitational wave tests are certainly more suitable to probe the gravitational sector itself and, in particular, are sensitive to the dynamical regime, which cannot be probed by electromagnetic tests.

Funding: This work was supported by the National Natural Science Foundation of China (NSFC), Grant No. 11973019, 12250610185, and 12261131497, the Natural Science Foundation of Shanghai, Grant No. 22ZR1403400, the Shanghai Municipal Education Commission, Grant No. 2019-01-07-00-07-E00035, and Fudan University, Grant No. JIH1512604.

Data Availability Statement: The models `relxill_nk` and `nkbb` are available on GitHub at <https://github.com/ABHModels> (accessed on 10 June 2023). Tests of the Kerr hypothesis with `relxill_nk` and `nkbb` have used data available on the HEASARC Data Archive website at <https://heasarc.gsfc.nasa.gov/docs/archive.html> (accessed on 10 June 2023).

Conflicts of Interest: The authors declare no conflict of interest.

References

1. Einstein, A. The foundation of the general theory of relativity. *Ann. Phys.* **1916**, *49*, 769–822. [[CrossRef](#)]
2. Will, C.M. The Confrontation between General Relativity and Experiment. *Living Rev. Relativ.* **2014**, *17*, 4. [[CrossRef](#)] [[PubMed](#)]
3. Dyson, F.W.; Eddington, A.S.; Davidson, C. A Determination of the Deflection of Light by the Sun's Gravitational Field, from Observations Made at the Total Eclipse of May 29, 1919. *Philos. Trans. R. Soc. Lond. A* **1920**, *220*, 291–333. [[CrossRef](#)]
4. Jain, B.; Khoury, J. Cosmological Tests of Gravity. *Ann. Phys.* **2010**, *325*, 1479–1516. [[CrossRef](#)]
5. Koyama, K. Cosmological Tests of Modified Gravity. *Rep. Prog. Phys.* **2016**, *79*, 046902. [[CrossRef](#)] [[PubMed](#)]
6. Ferreira, P.G. Cosmological Tests of Gravity. *Ann. Rev. Astron. Astrophys.* **2019**, *57*, 335–374. [[CrossRef](#)]

7. Abbott, B.P.; Abbott, R.; Abbott, T.; Abernathy, M.; Acernese, F.; Ackley, K.; Adams, C.; Adams, T.; Addesso, P.; Adhikari, R.; et al. Tests of general relativity with GW150914. *Phys. Rev. Lett.* **2016**, *116*, 221101; Erratum in *Phys. Rev. Lett.* **2018**, *121*, 129902. [[CrossRef](#)]
8. Yunes, N.; Yagi, K.; Pretorius, F. Theoretical Physics Implications of the Binary Black-Hole Mergers GW150914 and GW151226. *Phys. Rev. D* **2016**, *94*, 084002. [[CrossRef](#)]
9. Abbott, B.P.; Abbott, R.; Abbott, T.; Abraham, S.; Acernese, F.; Ackley, K.; Adams, C.; Adhikari, R.; Adya, V.; Affeldt, C.; et al. Tests of General Relativity with the Binary Black Hole Signals from the LIGO-Virgo Catalog GWTC-1. *Phys. Rev. D* **2019**, *100*, 104036. [[CrossRef](#)]
10. Bambi, C.; Freese, K.; Vagnozzi, S.; Visinelli, L. Testing the rotational nature of the supermassive object M87* from the circularity and size of its first image. *Phys. Rev. D* **2019**, *100*, 044057. [[CrossRef](#)]
11. Psaltis, D.; Medeiros, L.; Christian, P.; Özel, F.; Akiyama, K.; Alberdi, A.; Alef, W.; Asada, K.; Azulay, R.; Ball, D.; et al. Gravitational Test Beyond the First Post-Newtonian Order with the Shadow of the M87 Black Hole. *Phys. Rev. Lett.* **2020**, *125*, 141104. [[CrossRef](#)] [[PubMed](#)]
12. Vagnozzi, S.; Roy, R.; Tsai, Y.D.; Visinelli, L.; Afrin, M.; Allahyari, A.; Bambhaniya, P.; Dey, D.; Ghosh, S.G.; Joshi, P.S.; et al. Horizon-scale tests of gravity theories and fundamental physics from the Event Horizon Telescope image of Sagittarius A*. *arXiv* **2022**, arXiv:2205.07787
13. Cao, Z.; Nampalliwar, S.; Bambi, C.; Dauser, T.; Garcia, J.A. Testing general relativity with the reflection spectrum of the supermassive black hole in 1H0707-495. *Phys. Rev. Lett.* **2018**, *120*, 051101. [[CrossRef](#)] [[PubMed](#)]
14. Tripathi, A.; Nampalliwar, S.; Abdikamalov, A.B.; Ayzenberg, D.; Bambi, C.; Dauser, T.; Garcia, J.A.; Marinucci, A. Toward Precision Tests of General Relativity with Black Hole X-Ray Reflection Spectroscopy. *Astrophys. J.* **2019**, *875*, 56. [[CrossRef](#)]
15. Tripathi, A.; Zhang, Y.; Abdikamalov, A.B.; Ayzenberg, D.; Bambi, C.; Jiang, J.; Liu, H.; Zhou, M. Testing General Relativity with NuSTAR data of Galactic Black Holes. *Astrophys. J.* **2021**, *913*, 79. [[CrossRef](#)]
16. Bambi, C. Testing black hole candidates with electromagnetic radiation. *Rev. Mod. Phys.* **2017**, *89*, 025001. [[CrossRef](#)]
17. Bambi, C. *Black Holes: A Laboratory for Testing Strong Gravity*; Springer: Singapore, 2017; ISBN 978-981-10-4524-0. [[CrossRef](#)]
18. Chrusciel, P.T.; Costa, J.L.; Heusler, M. Stationary Black Holes: Uniqueness and Beyond. *Living Rev. Relativ.* **2012**, *15*, 7. [[CrossRef](#)]
19. Kerr, R.P. Gravitational field of a spinning mass as an example of algebraically special metrics. *Phys. Rev. Lett.* **1963**, *11*, 237–238. [[CrossRef](#)]
20. Bambi, C. Astrophysical Black Holes: A Compact Pedagogical Review. *Ann. Phys.* **2018**, *530*, 1700430. [[CrossRef](#)]
21. Bambi, C.; Malafarina, D.; Tsukamoto, N. Note on the effect of a massive accretion disk in the measurements of black hole spins. *Phys. Rev. D* **2014**, *89*, 127302. [[CrossRef](#)]
22. Kleihaus, B.; Kunz, J.; Radu, E. Rotating Black Holes in Dilatonic Einstein-Gauss-Bonnet Theory. *Phys. Rev. Lett.* **2011**, *106*, 151104. [[CrossRef](#)] [[PubMed](#)]
23. Giddings, S.B. Astronomical tests for quantum black hole structure. *Nat. Astron.* **2017**, *1*, 0067. [[CrossRef](#)]
24. Mottola, E. Gravitational Vacuum Condensate Stars. In *Regular Black Holes: Towards a New Paradigm of Gravitational Collapse*; Bambi, C., Ed.; Springer: Singapore, 2023.
25. Herdeiro, C.A.R.; Radu, E. Kerr black holes with scalar hair. *Phys. Rev. Lett.* **2014**, *112*, 221101. [[CrossRef](#)] [[PubMed](#)]
26. Herdeiro, C.; Radu, E.; Rúnarsson, H. Kerr black holes with Proca hair. *Class. Quantum Gravity* **2016**, *33*, 154001. [[CrossRef](#)]
27. Bambi, C. Testing Gravity with Black Hole X-Ray Data. In *Recent Progress on Gravity Tests*; Bambi, C., Cardenas-Avendano, A., Eds.; Springer: Singapore, 2024. [[CrossRef](#)]
28. Timmes, F.X.; Woosley, S.E.; Weaver, T.A. The Neutron star and black hole initial mass function. *Astrophys. J.* **1996**, *457*, 834. [[CrossRef](#)]
29. Bambi, C.; Brenneman, L.W.; Dauser, T.; Garcia, J.A.; Grinberg, V.; Ingram, A.; Jiang, J.; Liu, H.; Lohfink, A.M.; Marinucci, A.; et al. Towards Precision Measurements of Accreting Black Holes Using X-Ray Reflection Spectroscopy. *Space Sci. Rev.* **2021**, *217*, 65. [[CrossRef](#)]
30. Bambi, C. Testing General Relativity with black hole X-ray data: A progress report. *Arab. J. Math.* **2022**, *11*, 81–90. [[CrossRef](#)]
31. Ross, R.R.; Fabian, A.C. A Comprehensive range of x-ray ionized reflection models. *Mon. Not. R. Astron. Soc.* **2005**, *358*, 211–216. [[CrossRef](#)]
32. Garcia, J.; Kallman, T. X-ray reflected spectra from accretion disk models. I. Constant density atmospheres. *Astrophys. J.* **2010**, *718*, 695. [[CrossRef](#)]
33. Laor, A. Line profiles from a disk around a rotating black hole. *Astrophys. J.* **1991**, *376*, 90. [[CrossRef](#)]
34. Bambi, C.; Cardenas-Avendano, A.; Dauser, T.; Garcia, J.A.; Nampalliwar, S. Testing the Kerr black hole hypothesis using X-ray reflection spectroscopy. *Astrophys. J.* **2017**, *842*, 76. [[CrossRef](#)]
35. Novikov, I.D.; Thorne, K.S. Astrophysics of Black Holes. In *Black Holes*; DeWitt, C., DeWitt, B., Eds.; Gordon and Breach: New York, NY, USA, 1973.
36. Page, D.N.; Thorne, K.S. Disk-Accretion onto a Black Hole. Time-Averaged Structure of Accretion Disk. *Astrophys. J.* **1974**, *191*, 499–506. [[CrossRef](#)]
37. Davis, A.C.; Gregory, R.; Jha, R. Black hole accretion discs and screened scalar hair. *J. Cosmol. Astropart. Phys.* **2016**, *10*, 024. [[CrossRef](#)]

38. Bambi, C. Search for Variations of Fundamental Constants. In *Recent Progress on Gravity Tests*; Bambi, C., Cardenas-Avendano, A., Eds.; Springer: Singapore, 2024.
39. Bambi, C. Constraining possible variations of the fine structure constant in strong gravitational fields with the $K\alpha$ iron line. *J. Cosmol. Astropart. Phys.* **2014**, *3*, 34. [[CrossRef](#)]
40. Abdikamalov, A.B.; Ayzenberg, D.; Bambi, C.; Dauser, T.; Garcia, J.A.; Nampalliwar, S. Public Release of RELXILL_NK: A Relativistic Reflection Model for Testing Einstein's Gravity. *Astrophys. J.* **2019**, *878*, 91. [[CrossRef](#)]
41. Zhou, M.; Abdikamalov, A.B.; Ayzenberg, D.; Bambi, C.; Liu, H.; Nampalliwar, S. XSPEC model for testing the Kerr black hole hypothesis using the continuum-fitting method. *Phys. Rev. D* **2019**, *99*, 104031. [[CrossRef](#)]
42. Dauser, T.; Garcia, J.; Wilms, J.; Bock, M.; Brenneman, L.W.; Falanga, M.; Fukumura, K.; Reynolds, C.S. Irradiation of an Accretion Disc by a Jet: General Properties and Implications for Spin Measurements of Black Holes. *Mon. Not. Roy. Astron. Soc.* **2013**, *430*, 1694. [[CrossRef](#)]
43. García, J.; Dauser, T.; Lohfink, A.; Kallman, T.R.; Steiner, J.; McClintock, J.E.; Brenneman, L.; Wilms, J.; Eikmann, W.; Reynolds, C.S.; et al. Improved Reflection Models of Black-Hole Accretion Disks: Treating the Angular Distribution of X-rays. *Astrophys. J.* **2014**, *782*, 76. [[CrossRef](#)]
44. García, J.; Dauser, T.; Reynolds, C.S.; Kallman, T.R.; McClintock, J.E.; Wilms, J.; Eikmann, W. X-ray reflected spectra from accretion disk models. III. A complete grid of ionized reflection calculations. *Astrophys. J.* **2013**, *768*, 146. [[CrossRef](#)]
45. Roy, R.; Abdikamalov, A.B.; Ayzenberg, D.; Bambi, C.; Riaz, S.; Tripathi, A. Testing the weak-equivalence principle near black holes. *Phys. Rev. D* **2021**, *104*, 044001. [[CrossRef](#)]
46. Johannsen, T.; Psaltis, D. A Metric for Rapidly Spinning Black Holes Suitable for Strong-Field Tests of the No-Hair Theorem. *Phys. Rev. D* **2011**, *83*, 124015. [[CrossRef](#)]
47. Johannsen, T. Regular Black Hole Metric with Three Constants of Motion. *Phys. Rev. D* **2013**, *88*, 044002. [[CrossRef](#)]
48. Cardoso, V.; Pani, P.; Rico, J. On generic parametrizations of spinning black-hole geometries. *Phys. Rev. D* **2014**, *89*, 064007. [[CrossRef](#)]
49. Lin, N.; Tsukamoto, N.; Ghasemi-Nodehi, M.; Bambi, C. A parametrization to test black hole candidates with the spectrum of thin disks. *Eur. Phys. J. C* **2015**, *75*, 599. [[CrossRef](#)]
50. Ghasemi-Nodehi, M.; Bambi, C. Note on a new parametrization for testing the Kerr metric. *Eur. Phys. J. C* **2016**, *76*, 290. [[CrossRef](#)]
51. Konoplya, R.; Rezzolla, L.; Zhidenko, A. General parametrization of axisymmetric black holes in metric theories of gravity. *Phys. Rev. D* **2016**, *93*, 064015. [[CrossRef](#)]
52. Mazza, J.; Franzin, E.; Liberati, S. A novel family of rotating black hole mimickers. *J. Cosmol. Astropart. Phys.* **2021**, *04*, 082. [[CrossRef](#)]
53. Zhang, Y.; Abdikamalov, A.B.; Ayzenberg, D.; Bambi, C.; Nampalliwar, S. Tests of the Kerr hypothesis with GRS 1915+105 using different RELXILL flavors. *Astrophys. J.* **2019**, *884*, 147. [[CrossRef](#)]
54. Abdikamalov, A.B.; Ayzenberg, D.; Bambi, C.; Dauser, T.; Garcia, J.A.; Nampalliwar, S.; Tripathi, A.; Zhou, M. Testing the Kerr black hole hypothesis using X-ray reflection spectroscopy and a thin disk model with finite thickness. *Astrophys. J.* **2020**, *899*, 80. [[CrossRef](#)]
55. Tripathi, A.; Zhou, M.; Abdikamalov, A.B.; Ayzenberg, D.; Bambi, C.; Gou, L.; Grinberg, V.; Liu, H.; Steiner, J.F. Testing general relativity with the stellar-mass black hole in LMC X-1 using the continuum-fitting method. *Astrophys. J.* **2020**, *897*, 84. [[CrossRef](#)]
56. Tripathi, A.; Abdikamalov, A.B.; Ayzenberg, D.; Bambi, C.; Grinberg, V.; Zhou, M. Testing the Kerr Black Hole Hypothesis with GX 339-4 by a Combined Analysis of Its Thermal Spectrum and Reflection Features. *Astrophys. J.* **2021**, *907*, 31. [[CrossRef](#)]
57. Tripathi, A.; Abdikamalov, A.B.; Ayzenberg, D.; Bambi, C.; Grinberg, V.; Liu, H.; Zhou, M. Testing the Kerr black hole hypothesis with the continuum-fitting and the iron line methods: The case of GRS 1915+105. *J. Cosmol. Astropart. Phys.* **2022**, *01*, 019. [[CrossRef](#)]
58. Zhang, Z.; Liu, H.; Abdikamalov, A.B.; Ayzenberg, D.; Bambi, C.; Zhou, M. Testing the Kerr Black Hole Hypothesis with GRS 1716-249 by Combining the Continuum Fitting and the Iron-line Methods. *Astrophys. J.* **2022**, *924*, 72. [[CrossRef](#)]
59. Shashank, S.; Bambi, C. Constraining the Konoplya-Rezzolla-Zhidenko deformation parameters III: Limits from stellar-mass black holes using gravitational-wave observations. *Phys. Rev. D* **2022**, *105*, 104004. [[CrossRef](#)]
60. Akiyama, K.; Alberdi, A.; Alef, W.; Algaba, J.C.; Anantua, R.; Asada, K.; Azulay, R.; Bach, U.; Baczkowski, A.; Ball, D.; et al. First Sagittarius A* Event Horizon Telescope Results. VI. Testing the Black Hole Metric. *Astrophys. J. Lett.* **2022**, *930*, L17. [[CrossRef](#)]
61. Bambi, C. *Testing Fundamental Physics with Black Holes*, Talk Give at the "TianQin Astrophysics Workshop" (22–25 August 2022). Available online: <https://cosimobambi.github.io/research.html> (accessed on 17 June 2023).
62. Cardenas-Avendano, A.; Nampalliwar, S.; Yunes, N. Gravitational-wave versus X-ray tests of strong-field gravity. *Class. Quantum Gravity* **2020**, *37*, 135008. [[CrossRef](#)]
63. Abdikamalov, A.B.; Ayzenberg, D.; Bambi, C.; Nampalliwar, S.; Tripathi, A. Constraining the Konoplya-Rezzolla-Zhidenko deformation parameters: Limits from supermassive black hole x-ray data. *Phys. Rev. D* **2021**, *104*, 024058. [[CrossRef](#)]
64. Yu, Z.; Jiang, Q.; Abdikamalov, A.B.; Ayzenberg, D.; Bambi, C.; Liu, H.; Nampalliwar, S.; Tripathi, A. Constraining the Konoplya-Rezzolla-Zhidenko deformation parameters. II. Limits from stellar-mass black hole x-ray data. *Phys. Rev. D* **2021**, *104*, 084035. [[CrossRef](#)]
65. Tripathi, A.; Zhou, B.; Abdikamalov, A.B.; Ayzenberg, D.; Bambi, C. Constraints on Einstein-Maxwell dilaton-axion gravity from X-ray reflection spectroscopy. *J. Cosmol. Astropart. Phys.* **2021**, *7*, 002. [[CrossRef](#)]

66. Bambi, C.; Modesto, L.; Rachwał, L. Spacetime completeness of non-singular black holes in conformal gravity. *J. Cosmol. Astropart. Phys.* **2017**, *5*, 3. [[CrossRef](#)]
67. Bambi, C.; Modesto, L.; Porey, S.; Rachwał, L. Black hole evaporation in conformal gravity. *J. Cosmol. Astropart. Phys.* **2017**, *9*, 33. [[CrossRef](#)]
68. Chakrabarty, H.; Benavides-Gallego, C.A.; Bambi, C.; Modesto, L. Unattainable extended spacetime regions in conformal gravity. *J. High Energy Phys.* **2018**, *3*, 13. [[CrossRef](#)]
69. Zhou, M.; Cao, Z.; Abdikamalov, A.; Ayzenberg, D.; Bambi, C.; Modesto, L.; Nampalliwar, S. Testing conformal gravity with the supermassive black hole in 1H0707-495. *Phys. Rev. D* **2018**, *98*, 024007. [[CrossRef](#)]
70. Zhou, M.; Abdikamalov, A.B.; Ayzenberg, D.; Bambi, C.; Modesto, L.; Nampalliwar, S.; Xu, Y. Singularity-free black holes in conformal gravity: New observational constraints. *Europhys. Lett.* **2019**, *125*, 30002. [[CrossRef](#)]
71. Held, A.; Gold, R.; Eichhorn, A. Asymptotic safety casts its shadow. *J. Cosmol. Astropart. Phys.* **2019**, *6*, 029. [[CrossRef](#)]
72. Zhou, B.; Abdikamalov, A.B.; Ayzenberg, D.; Bambi, C.; Nampalliwar, S.; Tripathi, A. Shining X-rays on asymptotically safe quantum gravity. *J. Cosmol. Astropart. Phys.* **2021**, *1*, 47. [[CrossRef](#)]
73. Joshi, P.S.; Malafarina, D. Recent developments in gravitational collapse and spacetime singularities. *Int. J. Mod. Phys. D* **2011**, *20*, 2641–2729. [[CrossRef](#)]
74. Tao, J.; Riaz, S.; Zhou, B.; Abdikamalov, A.B.; Bambi, C.; Malafarina, D. Testing the δ -Kerr metric with black hole X-ray data. *arXiv* **2023**, arXiv:2301.12164
75. Quevedo, H.; Mashhoon, B. Exterior gravitational field of a rotating deformed mass. *Phys. Lett. A* **1985**, *109*, 13–18. [[CrossRef](#)]
76. Quevedo, H.; Mashhoon, B. Generalization of Kerr spacetime *Phys. Rev. D* **1991**, *43*, 3902. [[CrossRef](#)]
77. Kammoun, E.S.; Nardini, E.; Risaliti, G. Testing the accuracy of reflection-based supermassive black hole spin measurements in AGN. *Astron. Astrophys.* **2018**, *614*, A44. [[CrossRef](#)]
78. Shashank, S.; Riaz, S.; Abdikamalov, A.B.; Bambi, C. Testing Relativistic Reflection Models with GRMHD Simulations of Accreting Black Holes. *Astrophys. J.* **2022**, *938*, 53. [[CrossRef](#)]
79. Riaz, S.; Ayzenberg, D.; Bambi, C.; Nampalliwar, S. Reflection spectra of thick accretion discs. *Mon. Not. R. Astron. Soc.* **2020**, *491*, 417–426. [[CrossRef](#)]
80. Riaz, S.; Ayzenberg, D.; Bambi, C.; Nampalliwar, S. Modeling bias in supermassive black hole spin measurements. *Astrophys. J.* **2020**, *895*, 61. [[CrossRef](#)]
81. Zhang, S.; Santangelo, A.; Feroci, M.; Xu, Y.; Lu, F.; Chen, Y.; Feng, H.; Zhang, S.; Brandt, S.; Hernanz, M.; et al. eXTP—enhanced X-ray Timing and Polarimetry Mission. *Proc. SPIE Int. Soc. Opt. Eng.* **2016**, *9905*, 99051Q. [[CrossRef](#)]
82. Babak, S.; Gair, J.; Sesana, A.; Barausse, E.; Sopuerta, C.F.; Berry, C.P.L.; Berti, E.; Amaro-Seoane, P.; Petiteau, A.; Klein, A. Science with the space-based interferometer LISA. V: Extreme mass-ratio inspirals. *Phys. Rev. D* **2017**, *95*, 103012. [[CrossRef](#)]

Disclaimer/Publisher’s Note: The statements, opinions and data contained in all publications are solely those of the individual author(s) and contributor(s) and not of MDPI and/or the editor(s). MDPI and/or the editor(s) disclaim responsibility for any injury to people or property resulting from any ideas, methods, instructions or products referred to in the content.